# Fano Profiles on Multiphonon Continua in Electronic Transitions of Matrix-Isolated NO

M. Chergui[a] and N. Schwentner
*Institut für Experimentalphysik, Freie Universität Berlin, Arnimallee 14, D-1000 Berlin 33, Federal Republic of Germany*

V. Chandrasekharan
*Laboratoire de Photophysique Moléculaire, Centre National de la Recherche Scientifique, Université Paris-Sud, Bâtiment 213, F-91405 Orsay CEDEX, France*
(Received 2 November 1990)

Fano line shapes are reported in the excitation spectrum of the total fluorescence of NO trapped in Kr matrices. They result from the homogeneous configuration mixing of the sharp valence vibrational bands $B^2\Pi(v'=12,15,18)$-$X^2\Pi(v''=0)$ with the broadened multiphonon Rydberg vibrational bands $C^2\Pi(v'=0,1,2)$-$X^2\Pi(v''=0)$. The main features of the spectrum are reproduced by a simulation.

PACS numbers: 71.38.+i, 31.70.Dk, 33.70.Jg, 63.20.Kr

The interaction of a discrete level with a continuum gives rise to anomalous line shapes, in absorption experiments, which are known as Fano profiles.[1] The famous autoionization line profiles of autoionizing discrete states which are situated between the $\frac{3}{2}$ and $\frac{1}{2}$ ionization limits of rare-gas atoms are clear examples of Fano profiles.[2] Molecules may also exhibit such profiles as observed in the absorption of $N_2$ near 700 Å,[3] showing sharp minima in the ionization continuum. Predissociation also causes Fano line shapes in molecules as exemplified by the case of $H_2$.[4] In solids, the conduction band corresponds to the ionization continuum in atoms or molecules. The far-UV absorption spectrum of rare-gas solids exhibits line shapes which are similar to the gas-phase Fano line shapes, but are broadened and shifted slightly to higher energies.[5] Phonons provide another source of continuum states in solids. Acoustic modes are characterized by a continuous density of states up to the Debye frequency of the solid. Sharp lines may interfere with this continuum and lead to anomalous line shapes. To date, such examples concern $BaTiO_6$,[6] paraelectric crystals,[7] and solid HD near the ir $R_1(0)$ transition.[8] In all those cases,[5-8] the line shapes were qualitatively discussed in terms of interference effects, except for the case of solid HD (Ref. 8) for which a theoretical study was undertaken by Bose and Poll[9] and is still discussed.[8]

We recently investigated the spectroscopy and dynamics of the NO Rydberg states in rare-gas matrices. Rydberg absorption bands showed strong blueshifts (0.4–1.2 eV) and a FWHM (80–180 meV), increasing from Xe to Ne, as a result of the strong repulsive interaction of the Rydberg wave function with the surrounding matrix atoms.[10] The Rydberg vibrational bands appear as broad multiphonon continua with no detectable zero-phonon line. Indeed, large electron-phonon coupling strengths of $S=20$–$100$ were extracted from a line-shape analysis of the Rydberg absorption and emission bands.[11] On the other hand, vibrational bands of valence transitions are sharp, consisting of an intense zero-phonon line and a weaker phonon sideband, and are only slightly redshifted by a few meV with much weaker coupling strengths of $S=0.2$–$0.5$.[10,12] The Rydberg and valence states of NO lie in the same energy range, and in the gas phase, extensive Rydberg-valence configuration mixing occurs. The strongest is that between the Rydberg $C^2\Pi$ state and the valence $B^2\Pi$ state.[13] This mixing gives rise to perturbed spectroscopic features in absorption or emission.[13] In the solid, despite the strong broadenings and matrix shifts of NO Rydberg bands, the Rydberg-valence perturbations persist[10] and will be discussed in detail later. Here, however, we would like to present evidence for Fano line shapes resulting from discrete-line–multiphonon-continuum interactions in electronic transitions of NO in Kr matrices, namely, between the sharp $B^2\Pi(v',0)$ bands and the broad multiphonon $C^2\Pi(v,0)$ bands.

The samples were prepared by condensing krypton gas doped with 0.3% NO partial pressure on a cold LiF substrate ($T\simeq 6\pm 2$ K). Gases from Linde with purities of 99.998% for Kr and 99.9% for NO were used without further purification. The experimental setup was previously described.[10] Briefly, dispersed synchrotron light from the storage ring DORIS at DESY (Hamburg) was focused on the sample. The focus point serves as entrance slits to two secondary monochromators used to analyze the emitted light in the VUV and the UV–visible ranges. This arrangement enables us to record excitation spectra in which the secondary monochromator is set at a given emission wavelength or at zeroth order and the excitation wavelength is scanned. This gives a reproduction of the absorption spectrum provided all absorbing states contribute to emission with the same quantum efficiency. The advantage is that the background is now zero. This is the case here since the quantum efficiency for total luminescence is near unity and shows little wavelength dependence.[10,14]

When the ground state ($g$) has nonzero transition moments with two interacting states ($V$ and $R$), then an interference effect can occur in the transition from the $g$ to the $V$-$R$ mixed levels. Interference effects involving

 

discrete $R$ and $V$ levels appear as intensity transfer from the $g$-$V$ to the $g$-$R$ transition; the direction of the transfer depends on the "relative" signs of the transition moments and on the perturbation matrix elements.[13] For discrete-continuum interactions, an asymmetric line broadening occurs, characterized by Fano's index $q$, and the absorption cross section has the form[1]

$$\sigma_a(\varepsilon) = \sigma_R(q+\varepsilon)^2/(1+\varepsilon^2), \quad (1)$$

where

$$\varepsilon(E) = \frac{E - E_V}{\Gamma_V/2} \quad (2)$$

is the dimensionless energy offset from the line center $E_V$ of the valence band with FWHM $\Gamma_V$, and $\sigma_R$ corresponds to the continuum cross section. $q < 0$ results in a "window" on the high-frequency side of an absorption line, $q > 0$ on the low-frequency side, and $q = 0$ causes an absorption minimum on the continuum absorption background. $q$ is derived from

$$q = \frac{1}{\pi} \frac{\langle \phi_V|\boldsymbol{\mu}|\phi_g\rangle\langle\chi_V|\chi_g\rangle}{\langle \phi_R|\boldsymbol{\mu}|\phi_g\rangle\langle\chi_R|\chi_g\rangle} \frac{1}{\langle \phi_V|\mathbf{H}|\phi_R\rangle\langle\chi_V|\chi_R\rangle}, \quad (3)$$

where $\phi$ and $\chi$ are the electronic and vibrational wave functions, respectively. $\boldsymbol{\mu}$ is the dipole moment for the electronic transition from the ground state and $\langle \phi_V|\mathbf{H}|\phi_R\rangle$ is the electronic matrix element coupling the discrete state with the continuum state. Note that $q$ is dimensionless because $\langle\chi_V|\chi_R\rangle$ and $\langle\chi_R|\chi_g\rangle$ have units of (energy)$^{-1/2}$ and $\langle \phi_V|\mathbf{H}|\phi_R\rangle$ has units of (energy)$^{+1}$.

Figure 1 shows an excitation spectrum of the total fluorescence of NO in Kr matrices. Progressions of sharp bands appear superimposed on broad bands. The sharp bands belong to the valence progressions $B^2\Pi(v',0)$ and $B'^2\Delta(v',0)$,[10,12] whereas the broad bands were identified as the Rydberg progressions $A^2\Sigma^+$, $C^2\Pi$, and $D^2\Sigma^+(v',0)$.[10] The line profile of near-resonant $B(v',0)$ and $A(v',0)$ bands is not affected by their energy degeneracies [e.g., $B(4) \sim A(0), \ldots$]. This is not surprising as the $B$-$A$ configuration mixing is negligible.[15] The $C(v'=0\text{-}3,0)$ bands coincide with the $B(v'=12\text{-}18,0)$ bands and because of the strong configuration mixing between them, strong interference effects show up. Indeed, the broad $C(v',0)$ bands at $\sim 7$, $\sim 7.3$, and $\sim 7.6$ eV (indicated by hatched bars in Fig. 1) have a doublet structure, previously attributed to a site effect.[10] However, upon annealing the samples to 25 K, the doublet structure does not vanish, although site effects on the $A^2\Sigma^+$ state do disappear.[11] In fact, the minima at the center of the doublet correspond to Fano windows on the broad multiphonon $C(v',0)$ Rydberg bands, resulting from interaction with sharp $B(v',0)$ valence bands. A closer inspection shows that the $B(12,0)$ band sits on top of the $C(0,0)$ Rydberg band and its profile is typical of Fano line shapes with a sharp falloff on the high-energy side, giving a window on the continuum, as expected from negative $q$ values. $C(1)$ is in resonance with $B(15,0)$, but the latter has vanished and only a window shows up, typical of near-zero $q$ values. The $C(2,0)$ band is in resonance with $B(18,0)$, but also with $B'(2,0)$. No effect on the $B'(v,0)$ band profiles is expected as the $C$-$B$ mixing is negligible.[15] The doublet structure is not as clear in this case, but

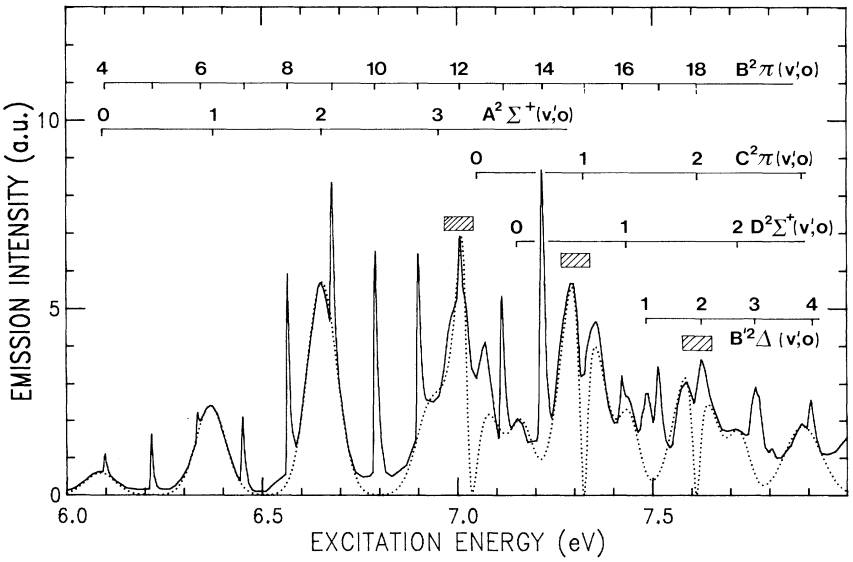


FIG. 1. Excitation spectrum of the total fluorescence of 0.3% NO in Kr matrices recorded at a resolution of $\Delta\lambda \simeq 0.5$ Å (solid line) and corrected for the wavelength dependence of the primary monochromator. The hatched bars are guides to the eye in order to distinguish the mixed $C$-$B$ Rydberg-valence bands. The dotted line represents the simulated spectrum (see text).

from the intensity of $B'(2,0)$ compared to that of higher $B'(v',0)$ bands, it is evident that the minimum or the low-energy side of the $B'(2,0)$ band is part of the window resulting from $B(18)$-$C(2)$ interaction.

A calculation of $q$ based on Eq. (3) is possible since all the parameters involved are known. They are given in Table I for all the pairs of levels involved. The overlap integrals have been calculated from Rydberg-Klein-Rees (RKR) potentials by Zumofen and Dressler.[16] The widths ($\Gamma_R$) and centers ($E_R$) of $C(v',0)$ bands were determined by fitting their wings, far from the interference region, with a Gaussian line shape. The FWHM is $\Gamma_R \approx 900$ cm$^{-1}$; thus the $\langle\chi_R|\chi_g\rangle$ and $\langle\chi_R|\chi_V\rangle$ overlap integrals should be divided by $0.93(900)^{1/2}$ cm$^{1/2}$ in order to yield the density of states in the center of the multiphonon bands. This is valid in a first approximation as the $B(v'=12,15,18)$ bands are located near the maxima of the $C(v'=0,1,2)$ bands (Fig. 1 and Table I). The Fano index thus estimated is also given in Table I. It qualitatively predicts the observed trends. Indeed for the $C(0)$-$B(12)$ interaction, $q$ is large and negative; thus an absorption line with a window on the high-energy side should occur, as actually observed. For the $C(1)$-$B(15)$ and $C(2)$-$B(18)$ interactions, $q$ lies near zero and only an absorption window should show up, again as actually observed.

Next, a simulation of the spectrum on the basis of Eqs. (1)–(3) was carried out. It should first be pointed out that Fano's theory[1] treats absorption spectra, and its extension to excitation spectra is justified by the fact that the quantum efficiency for total fluorescence of NO in Kr matrices near unity and shows negligible wavelength dependence.[10,14] In the Fano region, mixed $B$ and $C$ levels are probed and the quantum efficiency will not be strongly influenced by the mixing. This conclusion is confirmed by a comparison of Fig. 1 with the absorption spectrum of Ref. 17. Second, Eq. (1) is valid for a constant continuum, whereas in our case, its cross section exhibits a Gaussian energy dependence. This should introduce an energy-dependent $q$ factor which is taken as constant in the case of atoms because the lines are very sharp. Here the valence lines are $\approx 10$ times narrower than the Rydberg bands and surely $q$ depends on $E$. Since the $E$ dependence of $q$ has not been treated in the literature and is beyond the scope of this paper, we have taken a constant $q$ and modeled the continua by Gaussian profiles whose parameters (Table I) were determined as discussed above. The Gaussian parameters for the $A$ and $D(v',0)$ bands are the same as in Ref. 10. For the valence bands, we make the further approximation that the $B$ bands are Lorentzian line shapes having a FWHM $\Gamma_V \simeq 15$ meV, a value close to that measured by high- and medium-resolution absorption spectra.[10] For the fit, the free parameters are $q$ and $E_V$ (resonance center). The result of the simulation is shown by the dotted lines in Fig. 1 and the fit parameters ($q$,$E_V$) are given in Table I. The simulation reproduces qualitatively the experimental spectrum but the simulated Fano window is too deep. Varying $q$ modifies the profile but does not improve the fit in the window region, and the best fits were obtained for the $q$ values listed in Table I. The deviations in the window region can be due to several reasons. First, the energy dependence of $q$ was checked by introducing different linear and quadratic $q(E)$ dependences in our fit procedure. Although the shape of the Fano profile changes, the minimum in the window invariably goes to zero. Another possibility could be the nonzero lifetime of phonons making up the continuum. It has, however, been shown that the Fano theory holds for the case of a discrete phonon spectrum provided the lifetime broadening of the phonon states is sufficiently large to form a quasicontinuum.[18] We are left with the assumption of homogeneously broadened $C(v',0)$ bands as the most probable cause for the deviations. A superposition of Fano profiles resulting from interference with energetically close components in the inhomogeneous distribution of the $C(v',0)$ bands can explain the fact that the window does not go to zero. Already for the nearly spherical $3s\sigma$ orbital of the $A\,^2\Sigma^+$ state, a line narrowing of $\sim 10\%$ was observed upon annealing NO in Kr samples to 25 K,[11] and this should be even stronger for the $3p\pi$ orbital of the $C\,^2\Pi$ state. In addition, the $B(v',0)$ bands are not Lorentzian line shapes but have an asymmetric profile with a weak blue phonon sideband[10] and are surely inhomogeneously broadened.[10] In view of these approximations, we consider the fit of Fig. 1 satis-

TABLE I. Parameters describing the Rydberg-valence $C\,^2\Pi$-$B\,^2\Pi$ mixing and the resulting line shapes for NO in Kr matrices. The transition-matrix elements and the electronic coupling matrix element are given in a.u. (Ref. 13). $\langle\chi_a|\chi_b\rangle$ are the dimensionless overlap integrals calculated on the basis of RKR potentials (Ref. 16). $E_V$ and $E_R$ are the energies of the valence and Rydberg bands, respectively, and $\Gamma_V$ and $\Gamma_R$ are their FWHM. $q$ is the Fano index [Eq. (3)] and $I_R$ is the intensity (in the arbitrary units of Fig. 1) of $C(v',0)$ bands used in the fit.

| Mixed levels | $C(0)$-$B(12)$ | $C(1)$-$B(15)$ | $C(2)$-$B(18)$ |
|---|---|---|---|
| $\langle\phi_V\|\boldsymbol{\mu}\|\phi_g\rangle$ | −0.08 | −0.08 | −0.08 |
| $\langle\phi_R\|\boldsymbol{\mu}\|\phi_g\rangle$ | 0.31 | 0.31 | 0.31 |
| $\langle\phi_V\|\mathbf{H}\|\phi_R\rangle$ | 0.006 | 0.006 | 0.006 |
| $\langle\chi_V\|\chi_g\rangle$ | 0.214 | −0.225 | 0.22 |
| $\langle\chi_R\|\chi_g\rangle$ | 0.38 | 0.58 | 0.56 |
| $\langle\chi_R\|\chi_V\rangle$ | 0.013 | −0.076 | 0.16 |
| $q$ (calc.) | −2.1 | −0.25 | −0.1 |
| $q$ (fit) | −0.95 | −0.14 | −0.13 |
| $E_V$ (eV) | 7.023 | 7.32 | 7.615 |
| $E_R$ (eV) | 7.05 | 7.32 | 7.61 |
| $\Gamma_V$ (meV) | 15 | 15 | 15 |
| $\Gamma_R$ (meV) | 110 | 110 | 110 |
| $I_R$ | 5.0 | 7.3 | 4.2 |

fying.

In conclusion, we have presented evidence of Fano line shapes on multiphonon continua involving electronic transitions of NO in Kr solids. They result from interference effects between a sharp valence band and a broad multiphonon Rydberg band. The signs and absolute values of the Fano index $q$ qualitatively agree with the observed trends. The simulated spectrum reproduces the main features of the experimental spectrum but its quality is limited by approximations made for the simulation and by inhomogeneous broadening of experimental bands.

We are deeply indebted to Professor K. Dressler (Zürich) for pointing out to us the Fano features in our spectra and for discussions and encouragements and Dr. G. Zumofen (Zürich) for kindly providing us with the overlap integrals.

---

[a]Also at Laboratoire de Photophysique Moléculaire, CNRS, Université Paris-Sud, Bâtiment 213, F-91405 Orsay CEDEX, France.

[1]U. Fano, Nuovo Cimento **1**, 156 (1935); Phys. Rev. **124**, 1866 (1961).

[2]H. Beutler, Z. Phys. **93**, 177 (1935); R. P. Madden and K. Coddling, Phys. Rev. Lett. **10**, 516 (1963).

[3]R. E. Huffman, Y. Tanaka, and J. C. Larrebee, J. Chem. Phys. **39**, 910 (1963).

[4]M. Glass-Maujean, J. Breton, and P. M. Guyon, Chem. Phys. Lett. **63**, 591 (1979).

[5]R. Haensel, G. Keitel, C. Kunz, and P. Schreiber, Phys. Rev. Lett. **25**, 208 (1970).

[6]D. L. Rousseau and S. P. S. Porto, Phys. Rev. Lett. **20**, 1354 (1968).

[7]R. Blinc, J. R. Ferraro, and C. Postmus, J. Chem. Phys. **51**, 732 (1969).

[8]M. J. Clouter and A. R. W. Mc Kellar, Can. J. Phys. **65**, 1 (1987); A. R. W. Mc Kellar and M. J. Clouter, *ibid.* (to be published).

[9]S. K. Bose and J. D. Poll, Can. J. Phys. **65**, 1577 (1987).

[10]M. Chergui, N. Schwentner, and W. Böhmer, J. Chem. Phys. **85**, 2472 (1986); M. Chergui, Doctorate thesis, University of Paris, 1986 (unpublished).

[11]M. Chergui, N. Schwentner, and V. Chandrasekharan, J. Chem. Phys. **89**, 1277 (1988).

[12]E. Boursey and J.-Y. Roncin, J. Mol. Spectrosc. **55**, 31 (1975).

[13]R. Galusser and K. Dressler, J. Chem. Phys. **76**, 4311 (1982), and references therein.

[14]M. Chergui and N. Schwentner, J. Chem. Phys. **91**, 5993 (1989).

[15]E. Miescher and K. P. Huber, *International Review of Science, Physical Chemistry (2)* (Butterworths, London, 1976), Vol. 3, p. 37.

[16]G. Zumofen and K. Dressler (private communication).

[17]E. Morikawa, A. M. Köhler, R. Reininger, V. Saile, and P. Laporte, J. Chem. Phys. **89**, 2729 (1988).

[18]E. Kyrölä and J. H. Eberly, J. Chem. Phys. **82**, 1841 (1985).